Available online at www.sciencedirect.com
ScienceDirect
International Journal of Mass Spectrometry 267 (2007) 167–182
International Journal of Mass Spectrometry
www.elsevier.com/locate/ijms

A critical evaluation of the experimental and theoretical determination of lithium cation affinities☆

M.T. Rodgers [a], P.B. Armentrout [b,*]

[a] *Department of Chemistry, Wayne State University, Detroit, MI 48202, USA*
[b] *Department of Chemistry, University of Utah, Salt Lake City, UT 84112, USA*

Received 13 November 2006; received in revised form 18 January 2007; accepted 20 February 2007
Available online 25 February 2007

Abstract

A comprehensive comparison of multiple levels of theory with experimental values for about thirty lithium cation affinities (LCAs) is conducted. The experimental values are largely taken from threshold collision-induced dissociation (TCID) measurements augmented with equilibrium measurements from ion cyclotron resonance experiments. Possible reasons for errors in the experimental TCID results are explored. An examination of the theoretical results reveals that core correlation on the lithium ion(Li-C) is needed to accurately describe these complexes. Several procedures for assessing complete basis set (CBS) extrapolations from MP2(full)/aug-cc-pVnZ(Li-C)//MP2(full)/cc-pVDZ(Li-C), n = D, T, and Q, calculations are completed and compared to experiment and lower levels of theory. It is found that LCAs calculated using CBS methods including core correlation are higher than most other methods and generally in good agreement with experimental values. Because the CBS approach requires use of the computationally intensive aug-cc-pVQZ(Li-C) basis set, we recommend that an adequate level of theory is provided by a MP2(full)/aug-cc-pVTZ(Li-C)//MP2(full)/cc-pVDZ(Li-C) approach excluding basis set superposition errors. Given these theoretical results, discrepant experimental values in the literature for several lithium ion complexes are evaluated.

Keywords: Collision-induced dissociation; Complete basis set extrapolation; Core correlation; Guided ion beams; Lithium cation affinities

1. Introduction

During the last decade, substantial progress has been made in the measurement of alkali metal cation affinities for increasingly complex molecules. These developments have been driven by the interest in understanding fundamental aspects of such metal ion interactions and in particular with biologically relevant molecules. Synergistically, theoretical methods have developed to the point of being an equal partner with experiment in exploring trends in these binding energies, while simultaneously characterizing their structures. In previous work [1], we compared experimental results for sodium cation affinities to a number of levels of theory, finding very good agreement for several levels of theory of both modest and advanced computational effort. In contrast, theoretical results for lithium cation affinities (LCAs) are often lower than experiment by more than the experimental error. At first glance, these results appear counterintuitive because lithium is the smallest alkali metal cation. However, lithium cations have the highest charge density (such that they exhibit the shortest metal–ligand bond lengths), making them more challenging computationally as perturbations of the ligands are much more extensive than for the heavier alkali metal cations. Further, the low mass of the lithium cation also makes them more challenging experimentally. It is the purpose of this paper to investigate both experimental and theoretical origins for the discrepancies in the experimental and theoretical LCAs. This analysis allows us to recommend appropriate levels of theory to achieve the most accurate results along with a less intensive computational approach that can provide adequate accuracy for larger systems or for studies where only limited resources are available.

In the present work, we restrict our investigation to interactions between lithium cations and a single ligand. Experimentally, such LCAs have been measured for a wide range of ligands, ranging from very weak interactions of Ar to very strong interactions of crown ethers. Our own guided ion beam

☆ In memory of Sharon Lias and her many contributions to ion thermochemistry.

* Corresponding author. Tel.: +1 801 581 7885; fax: +1 801 581 8433.
E-mail address: armentrout@chem.utah.edu (P.B. Armentrout).

1387-3806/$ – see front matter © 2007 Elsevier B.V. All rights reserved.
doi:10.1016/j.ijms.2007.02.034

mass spectrometry (GIBMS) studies provide the only absolute determinations of LCAs by measuring the energy threshold for collision-induced dissociation (CID) processes, reactions (1) [2–26].

$$Li^+(L) + Xe \rightarrow Li^+ + L + Xe \quad (1)$$

Previously, ion cyclotron resonance (ICR) mass spectrometry (MS) studies by Woodin and Beauchamp provided relative lithium cation basicities (LCBs), the free energy equivalent of the LCA [27]. Their work included molecules such as H_2O, CH_3OH, CH_3OCH_3, NH_3, CH_3NH_2, and C_6H_6. The LCBs were placed on an absolute scale using a value for $D(Li^+\text{-}OH_2)$ from Džidić and Kebarle [28], which had not been measured but instead had been extrapolated from measured values for larger $Li^+(H_2O)_x$ complexes, $x = 2$–6. The most comprehensive examination of LCBs comes from the classic studies of Taft and coworkers using ICR MS [29]. Originally, these were anchored to the value for $D(Li^+\text{-NH3})$ taken from Woodin and Beauchamp, but the relative values have been reanchored [30] at our suggestion using a G2 [31] theoretical value for $D_0(Li^+\text{-}OH_2)$, chosen because it agrees with our measurement [4]. Finally, Bojesen, Wesdemiotis, Gronert, and coworkers have used the kinetic method to examine the relative binding energies of amino acids and nucleobases [32–34]. The present work focuses on a limited set of molecules for which GIBMS values exist along with several additional small molecules for which studies have not yet been performed. These experimental values are augmented with relative values from Taft's work, after using theory to adjust the ΔG values to ΔH_0.

Previous computational studies of lithium cation affinities also abound and are too numerous to cite comprehensively. Several theoretical studies are notable and almost all preceded a comprehensive experimental data set for comparison. Del Bene has provided many studies of LCAs, primarily of small molecules but including nucleobases [35]. In 1996 [36], she utilized the Dunning correlation-consistent polarized split-valence basis sets (cc-pVnZ, where n = D for double, T for triple, and Q for quadruple zeta) [37] and augmented with diffuse functions on atoms other than H and Li (aug'-cc-pVnZ) at the MP4 level of theory (found to be convergent compared to CCSD(T) calculations). She found that diffuse functions lower the computed LCAs, reducing the basis set superposition error (BSSE) and yielding satisfactory convergence at aug'-cc-pVTZ. In 1998, Remko et al. [38] used the complete basis set extrapolation method (CBS-Q) developed by Petersson and coworkers [39] to study LCAs relative to proton and Mg^{2+} affinities of a series of simple molecules. Siu et al. [40] examined the G2 [31] and G3 [41] Gaussian protocols for predicting Li^+, Na^+, and K^+ binding affinities, recommending that geometry corrected counterpoise calculations be adopted for the LCAs.

The binding energy of Li^+ to benzene is one of the best studied cases computationally. Nicholas et al. [42] found that MP2/6-311 + G^* results including counterpoise corrections for BSSE were well converged with regard to the extent of electron correlation (compared with CCSD(T) calculations), yielding a LCA of 146 kJ mol^{-1}, but that further increases in basis set size did increase the LCA. In a later study [43], this latter effect was more thoroughly investigated using complete basis set (CBS) extrapolations. It was concluded that the CBS limit (154 kJ mol^{-1}) was found to lie closer to the raw binding energies than to values corrected for BSSE. Core/valence and higher order correlation effects were estimated via CCSD(T) calculations and found to be small. Vollmer et al. [44] calculated the LCA of benzene at the G3(MP2) [45] level, obtaining a value of 144 kJ mol^{-1}. The best of these values, the CBS result, lies between the experimental values of 161.1 ± 13.5 kJ mol^{-1} from GIBMS studies [9] and the ICR MS results of ∼150 kJ mol^{-1} [27,30].

2. Experimental data

The experimental data used in the evaluations of this paper are taken largely from GIBMS CID studies conducted in our research groups. This covers a very wide range of ligand strengths, from weakly bound species (e.g., Ar and CO [6]) to very strongly bound bidentate (e.g., proline [24] and ethanol amine, $HOC_2H_4NH_2$ [25]) and tetradentate (12-crown-4 [3]) ligands. In all cases, the thermochemistry is presented as 0 K bond dissociation energies or enthalpies of dissociation, i.e., LCAs. In order to augment this data set, values derived from the ICR MS equilibrium studies of Woodin and Beauchamp [27] and Taft and coworkers [29,30] are also examined. However, the ICR values need to be adjusted from free energies at 298 [27] or 373 [29,30] K to 0 K, which can be done using the theoretical results obtained here. Difficulties with this procedure include the proper handling of hindered rotors. Table 1 shows ΔG_{298} values taken from Woodin and Beauchamp along with $T\Delta S_{298}$ and $(\Delta H_{298} - \Delta H_0)$ corrections calculated using rigid rotor and harmonic oscillator approximations from the MP2(full)/cc-pVDZ(Li-C) level of theory (see description below). The ΔG_{373} values from Taft and coworkers are also shown along with the appropriate thermal corrections, $T\Delta S_{373}$ and $(\Delta H_{373} - \Delta H_0)$, calculated using the same approach. The thermal corrections given here differ appreciably in most cases from those presented by Woodin and Beauchamp who estimated the rotational and vibrational corrections because they did not have access to results specific to each complex. In the present work, uncertainties in the thermal corrections are estimated from 10% uncertainties in all vibrational frequencies and rotational constants except for the three metal–ligand motions, where factors of two uncertainties in the vibrational frequencies are used. Because the Taft data was recently reanchored using our value for $D_0(Li^+\text{-}OH_2)$ [30], these ΔG_{373} free energies can be used directly, but the ΔG_{298} values from Woodin and Beauchamp were anchored to the Džidić and Kebarle extrapolated value for $D_0(Li^+\text{-}OH_2)$ [28]. Hence, these values are reanchored by minimizing the deviations from the results of Taft and coworkers after both data sets are corrected to 0 K enthalpies. In the six cases included here from Woodin and Beauchamp, the agreement with the results from Taft and coworkers is good, with deviations less than 2.5 kJ mol^{-1}.

In Table 1, the thermal corrections are obtained by treating all torsional motions as vibrations. This may not be correct, however, as internal rotors may be influenced dramatically

Table 1
Experimental lithium cation affinities at 0 K in kJ mol^{-1} [a]

	ICR[b]				GIBMS[c]	KM[d]
	ΔG_T	$T\Delta S_T$[e]	$(\Delta H_T - \Delta H_0)$[e]	ΔH_0[f]	ΔH_0[f]	
Ar					**32.8 (13.5)**[g]	
NO					**59.8 (10.0)**[h]	
CO					**55.0 (12.5)**[g]	
H_2O	103.3 (8.4), 112.8 (14.3)[i]	35.4 (5.6), 28.0 (4.2)	4.3 (2.4), 4.1 (2.0)	134.4 (10.4), 136.7 (13.5)	**133.1 (13.5)**[j]	
CH_3OH	119.2 (8.4), 125.4 (14.3)[i]	35.4 (6.0), 28.2 (4.7)	2.4 (1.6), 2.4 (1.3)	152.1 (10.4), 151.2 (15.1)	**155.0 (8.5)**[k]	
C_6H_6	112.6 (8.4), 122.8 (14.3)[i]	40.0 (5.8), 31.8 (4.6)	3.2 (1.6), 3.1 (1.7)	149.4 (10.3), 151.5 (15.1)	161.1 (13.5)[l]	
CH_3OCH_3	123.4 (8.4), 129.5 (14.3)[i]	36.0 (6.3), 27.9 (5.0)	1.9 (1.3), 1.8 (1.1)	157.5 (10.6), 155.6 (15.2)	**165.0 (10.6)**[m]	
NH_3	126.4 (8.4), 132.9 (14.3)[i]	37.6 (5.3), 29.8 (3.9)	4.9 (2.5), 4.6 (2.0)	**159.1 (10.3)**, 158.1 (15.0)		
C_2H_5OH	127.2 (8.4)	36.6 (6.2)	2.3 (1.3)	161.5 (10.3)	**163.5 (6.5)**[k]	
CH_3NH_2	131.0 (8.4), 137.9 (14.3)[i]	37.7 (5.9), 30.2 (4.5)	3.2 (1.8), 3.2 (1.5)	**165.5 (10.4)**, 164.9 (15.1)		
CH_3CHO	133.0 (8.4)	35.2 (6.2)	1.9 (1.1)	**166.3 (10.6)**		
$C_2H_5CO_2H$	131.2 (8.7)	39.2 (6.2)	2.6 (0.9)	167.8 (10.7)	**165.0 (6.0)**[n]	
$C_2H_5CO_2CH_3$	136.8 (8.4)					
1-C_3H_7OH	131.4 (8.4)	41.1 (6.2)	3.4 (1.3)	169.1 (10.5)	**170.3 (8.6)**[k]	
2-C_3H_7OH	135.1 (8.4)	36.9 (6.3)	2.1 (1.1)	169.9 (10.5)	**172.8 (7.5)**[k]	
Pyrrole					**177.4 (16.6)**[o]	
C_6H_5OH	120.8 (8.7)	42.1 (6.1)	3.1 (1.6)	159.8 (10.7)	178.5 (16.1)[p]	
$C_6H_5OCH_3$	126.4 (8.4)					
Pyridine	146.4 (8.4)	37.7 (6.1)	2.2 (1.4)	182.0 (10.5)	**181.0 (14.5)**[q]	
CH_3COCH_3	147.7 (8.4)	36.9 (6.3)	2.0 (0.8)	**182.6 (10.5)**		
$CH_3COC_2H_5$	150.6 (8.4)	38.6 (6.3)	2.1 (0.8)	187.2 (10.5)	**190.1 (7.0)**[n]	
1-$C_3H_7NH_2$					**197.8 (6.0)**[n]	
Imidazole	159.4 (8.4)	38.1 (6.0)	2.4 (1.5)	195.1 (10.4)	210.8 (9.5)[r]	
Uracil					**211.5 (6.1)**[s]	211 (12)[t]
Glycine					**220.0 (8.0)**[n]	213 (12)[u]
Adenine					**226.1 (6.1)**[s]	226 (12)[t]
$(CH_3)_2NCHO$	173.6 (8.4)	37.2 (6.3)	2.2 (1.2)	**208.5 (10.6)**		
$2NH_2$pyridine					**237.8 (21.1)**[v]	
$(CH_3OCH_2)_2$	187.9 (8.4)	45.0 (6.3)	3.9 (1.2)	229.0 (10.6)	241.2 (18.3)[w]	
Proline					**278.8 (9.7)**[x]	229 (13)[y]
$HOC_2H_4NH_2$					**289.5 (9.0)**[n]	
12-crown-4					**371.5 (51)**[w]	

[a] Uncertainties in parentheses.
[b] Except as noted, ion cyclotron resonance (ICR) mass spectrometry values are from Taft and coworkers [29,30]. $T = 373$ K.
[c] Guided ion beam mass spectrometry results.
[d] Kinetic method results.
[e] Thermal corrections calculated using the rigid rotor harmonic oscillator approximation with vibrational frequencies and rotational constants calculated at the MP2(full)/cc-pVDZ(Li-C) level. Frequencies scaled by 0.9646.
[f] Values in bold face are used as the experimental data set for comparison to theory.
[g] Ref. [6].
[h] Ref. [26].
[i] ICR values from Woodin and Beauchamp [27], adjusted as described in the text. $T = 298$ K.
[j] Ref. [4]. [k]Ref. [5]. [l]Ref. [9]. [m]Ref. [2]. [n]Ref. [25]. [o]Ref. [13]. [p]Ref. [16]. [q]Ref. [11]. [r]Ref. [7]. [s]Ref. [8]. [t]Ref. [33]. [u]Ref. [32]. [v]Ref. [12]. [w]Ref. [3]. [x]Ref. [24]. [y]Ref. [34].

by complexation with the lithium cation. Examination of the motions for Li^+ (alcohol) complexes indicates that the lithium cation increases the vibrational frequencies calculated for these motions. In an extreme limit, one can imagine that the torsions should be treated as a free or hindered rotor in the free ligand and as a vibration in the complex. To gauge how the treatment of the torsional motions might influence the resulting LCAs, thermal corrections for methanol and ethanol were also calculated assuming free rotors in the ligand. The $T\Delta S_{373}$ and $\Delta H_{373} - \Delta H_0$ values are 39.3 and 2.3 kJ mol^{-1} for methanol and 46.3 and 1.8 for ethanol, such that the overall effect on converting from ΔG_{373} to ΔH_0 is an increase of 4–5 kJ mol^{-1} per torsional mode. If a hindered rotor is assumed for free methanol, the values change to 32.5 and 0.8 kJ mol^{-1}, respectively, such that the overall effect on converting from ΔG_{373} to ΔH_0 is a decrease of about 1 kJ mol^{-1}. These changes are likely to be upper limits to the true effects, but indicate that systematic errors of several kJ mol^{-1} per torsional mode may be introduced by the thermal corrections.

There are twelve systems where values are available from both ICR and GIBMS studies. For eight of these systems (H_2O, CH_3OH, CH_3OCH_3, C_2H_5OH, 1-C_3H_7OH, 2-C_3H_7OH, pyridine, and $CH_3COC_2H_5$,), the agreement is quite good, as shown in Fig. 1, with a mean absolute deviation (MAD) of 2.7 ± 2.1 kJ mol^{-1}. Of course, this is partially because the ICR values have been put on an absolute scale essentially

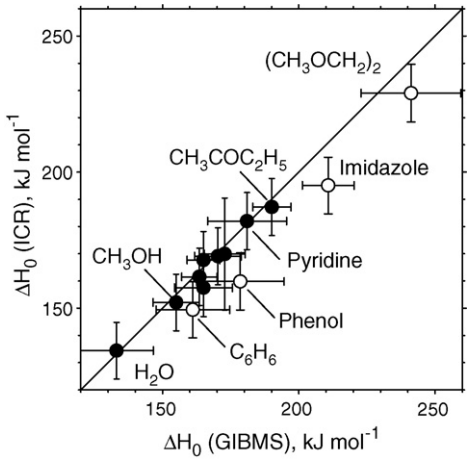

Fig. 1. Comparison of LCAs measured using threshold CID in a GIBMS and those derived from ICR equilibrium measurements. All values are 0 K enthalpies from Table 1. Most compounds are labeled by the ligand. The unlabeled overlapping group in the middle includes CH_3OCH_3, $C_2H_5CO_2H$, and three alcohols. Open symbols indicate the four values for which GIBMS and ICR results do not agree well, benzene, phenol, imidazole, and dimethoxyethane.

using our value for $D_0(Li^+\text{-}H_2O)$ [4]. Nevertheless, the agreement is gratifying. For three systems, benzene, imidazole, and dimethoxyethane, $(CH_3OCH_2)_2$, the discrepancies between the GIBMS and ICR values are larger, 11.7, 15.7, and 12.2 kJ mol^{-1}, although still within the combined experimental errors. Two other values where related compounds are available in the two studies are for $C_2H_5CO_2X$ and C_6H_5OX, where X = H for the GIBMS studies and X = CH_3 for the ICR studies. In these two cases, the ΔG_{373} values are approximately adjusted for the methyl group by subtracting 5.6 kJ mol^{-1}, the average difference between methyl additions in the alcohols and ketones. The adjusted ΔH_0 value obtained for $C_2H_5CO_2H$ agrees well with the GIBMS value, 167.8 versus 165.0 kJ mol^{-1}, whereas that for phenol, 159.8 kJ mol^{-1}, is 18.7 kJ mol^{-1}, lower than the GIBMS value of 178.5 kJ mol^{-1} [14].

A couple of additional experimental values from the literature are also included in Table 1. These are all determined from kinetic method experiments, such that they rely on having adequate reference species. Bojesen et al. [32] measured the LCA (temperature unspecified) of glycine using dimethylformamide, $(CH_3)_2NCHO$, as a reference, but never mention where this reference value came from (although it appears consistent with the ΔH_0 value derived from Burk et al. [30] in Table 1). This value is slightly below the GIBMS value and within experimental uncertainties. (Although Bojesen et al. do not assign an uncertainty to their value, the uncertainty provided in Table 1 is taken from the uncertainty in the dimethylformamide reference value and includes a 4 kJ mol^{-1} uncertainty in the relative values.) Cerda and Wesdemiotis [33] measured the LCAs of the nucleobases, including adenine and uracil, but use a reference value for glycine taken from Bojesen et al. [32]. Hence, their cited relative uncertainties of 4 kJ mol^{-1} have been increased by including the uncertainty in the reference value. These two kinetic method values are in very good agreement with the GIBMS values [8], Table 1. Feng et al. [34] have reported an experimental ΔG_{298} value for Li^+ (Pro) of 199 ± 13 kJ mol^{-1} obtained via the kinetic method using LCBs of dimethylformamide, methylacetamide, and dimethylacetamide reported by Burk et al. [34] as reference species. This value is 49 ± 17 kJ mol^{-1} lower than our reported ΔG_{298} value of 248 ± 11 kJ mol^{-1}.

In the remainder of this paper, the experimental data set used for a critical evaluation of the theoretical results is provided by the GIBMS values excluding the four cases where discrepancies with the ICR results are observed: benzene, phenol, imidazole, and $(CH_3OCH_2)_2$ (although these four systems are then discussed once an appropriate level of theory is identified). Because of the uncertainties introduced by the thermal corrections, the GIBMS values at 0 K are preferred in the eight cases where ICR values are also available. These data are then augmented by ICR results for systems where GIBMS studies have not yet been performed, NH_3, CH_3NH_2, CH_3CHO, $(CH_3)_2CO$, and $(CH_3)_2NCHO$. None of the kinetic method results are included as the temperature is ill-defined and three of the four values agree with GIBMS values anyway. Overall, this provides a set of 26 systems to help evaluate various theoretical approaches.

3. Experimental Issues

As noted above, the difficulty that lithium cations present experimentally is their low mass to charge ratio, which could potentially have several effects that could lead to lower sensitivity in CID measurements. (1) The low mass of lithium compared to most ligands of interest means that the relative velocity of the lithium cation fragment is higher than for heavier alkali metal cations. These high relative velocities could mean that lithium cations are not trapped as effectively in the octopole ion beam guide used to collect the product ions in the collision region of our GIBMS instruments [46]. (2) In addition (and more likely), these high relative velocities may limit the transmission efficiency through the quadrupole mass filters used to analyze the products. In actuality, neither effect should lead to shifts in the observed thresholds because the relative velocities of the product ions at threshold are zero, such that the products must have a velocity in the laboratory frame equal to the velocity of the center of mass of the reactants, which is well focused and forward scattered, in all but the lightest Li^+(L) systems. However, such effects may restrict the collection of Li^+ products at higher collision energies, thereby distorting the shape of the cross-section such that routine analysis of the cross-sections could lead to thresholds higher than the thermodynamic limit. In previous studies, such effects have been minimized by carefully tuning the rf voltages applied to the octopole and by reducing the mass resolution of the quadrupole mass filter to maximize transmission without sacrificing the ability to separate Li^+ and Li^+(L). Such problems have therefore been minimized in our previous work although this cannot be eliminated as a potential source of experimental difficulties.

Another possible difficulty with the lithium cation complexes relates to the dynamics of the dissociation process. Because the interactions of Li^+ with ligands are much stronger than the heavier alkali metal cations, it is conceivable that our use of a loose (phase space limit) transition state to model the dissocia-

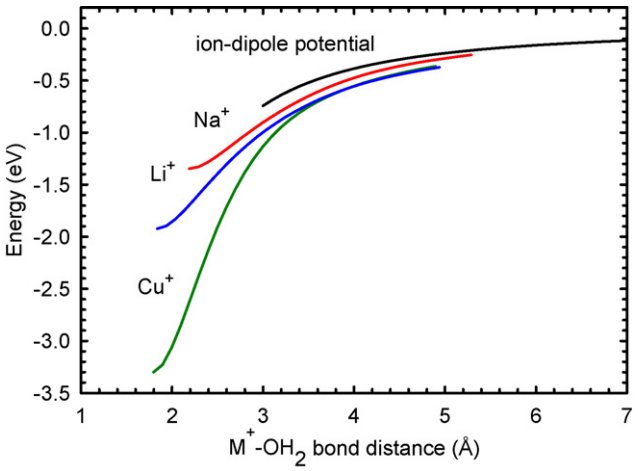

Fig. 2. Calculated potential energy curves for the interaction of Cu^+, Li^+, and Na^+ with H_2O as a function of the metal cation–oxygen bond distance relative to separated $M^+ + H_2O$. The black line shows the long-range ion–dipole interaction.

tion behavior [47] is inappropriate and that a tighter transition state should be used. The light mass of lithium also affects the dissociation dynamics because this changes the orbital angular momentum of the dissociation products. The latter effect should be fully accounted for in the model developed for our CID studies, but the choice of transition state has only been systematically evaluated for a small subset of ligands (the C_1–C_4 alcohols) [5]. To investigate the choice of transition state further, potential energy surfaces as a function of internuclear distance for interaction of Li^+ with several molecules (H_2O, NH_3, $(CH_3)_2O$, $(CH_3)_2CO$, and imidazole) were calculated at the B3LYP/6-31G(d) level of theory. Comparable calculations were also performed for the corresponding Na^+ and Cu^+ systems, where experiment and theory agree reasonably well, but where the metal cation affinities bracket those of Li^+, i.e., $Na^+ < Li^+ < Cu^+$. In all cases, these are relaxed potential energy surface scans that allow the ligand to change geometry as the metal cation recedes. Results for water, which are typical of all five ligand systems, are shown in Fig. 2. This figure shows that the general behavior of all three metals is identical at long range, with deviations only near the minimum. Also shown in Fig. 2 is the point charge — dipole potential, $V = -\mu e r^{-2}$, where μ is the dipole moment, e is the charge on the electron, and r is the metal cation–oxygen bond distance. It can be seen that the potential energy surfaces at long range all parallel this simple potential, as might be expected. Again, parallel behavior is obtained for all five ligands examined here. As our phase space model for the loose transition state uses such potentials as the basis for location of the transition state, the calculated potential energy surfaces suggest that our choice of transition state should not be an issue for lithium compared to the other metal cations.

4. Theoretical issues

All calculations are performed using the Gaussian03 suite of programs [48]. For most of the smaller complexes, generally up to five or six heavy atoms, the calculations could be performed on high performance personal computers, whereas calculations for larger complexes often used either the CHPC supercomputing cluster at Utah or the high performance Grid computing system at Wayne State. The larger complexes examined here could not have been performed without the supercomputing facilities, and even these are presently unable to perform the largest calculations for the Li^+(12-crown-4) system.

4.1. Conventional approaches

Table 2 compares experimental values for LCAs to those calculated at the levels of theory examined in our previous study of sodium cation affinities [1]. These include MP2(full) and several levels of density functional theory (B3LYP [49,50], B3P86 [49,51], and MPW1PW91 [52]). At each of these chosen levels of theory, geometry optimizations and vibrational frequency analyses are performed using the 6-31G(d, p) basis set followed by single point calculations using 6-311 + G(2d, 2p). MP2(full)/6-311 + G(2d, 2p)//B3LYP/6-31G(d, p) calculations are also included. Corrections for zero point energies (ZPE) [53] and for BSSE at the full counterpoise level [54,55] are included in all values. In addition, the complete basis set extrapolation approaches (CBS-4M, CBS-Q, and CBS-QB3) [39] and the Gaussian composite protocols (G2 [31] and G3 [41]) for accurate thermochemistry are included.

Comparison of the various theoretical values to the experimental results is facilitated by the mean absolute deviations (MADs) between experiment and theory shown at the bottom of the table. The MADs, which are comparable to the experimental uncertainties, have fairly sizable uncertainties indicating that the discrepancies are not a systematic additive effect. The simple approaches generally do not perform very well, with B3LYP and MPW1PW91 giving the best results. [It should be noted that the MPW1PW91 results in Table 2 are for the corrected version of the MPW exchange functional implemented in Gaussian03. Gaussian98 uses a version in which a local scaling factor was applied in computing the non-local correction. The incorrect version gave results that were systematically higher than the correct version by an average of 0.83 ± 0.56 kJ mol^{-1} (25 values excluding uracil, pyrrole, pyridine, and aminopyridine) with a maximum deviation of 2.38 kJ mol^{-1} for 1-$C_3H_7NH_2$.] The CBS-4M, CBS-Q, and CBS-QB3 approaches also fail to yield adequate results, whereas the best performance is observed for G3. Interestingly, if counterpoise corrections for BSSE are not included for the MP2 and MP2/B3LYP calculations, the agreement with experiment improves, yielding MADs of 8.1 ± 6.9 kJ mol^{-1} and 9.2 ± 8.2 kJ mol^{-1}, respectively. In contrast, eliminating the counterpoise corrections for the B3LYP approach, which are already much smaller than for the MP2 approaches, has little effect, yielding a MAD of 10.0 ± 7.3 kJ mol^{-1}. On the basis of the results in Table 2, it is apparent that the theoretical approaches previously successful for other alkali metal cations are insufficient for lithium cations.

4.2. Core correlation

As pointed out in the introduction, lithium cations differ from heavier alkali metal cations primarily in being much smaller. The

Table 2
Experimental and calculated lithium cation affinities at 0 K in kJ mol^{-1}

Ligand	Experiment[a]	Theory									
		MP2(full)[b]	MP2(full)// B3LYP[b]	B3LYP[b]	B3P86[b]	MPW1 PW91[b]	CBS-4M	CBS-Q	CBS-QB3	G2	G3
Ar	32.8 (13.5)	22.1	22.2	26.3	22.5	24.5	18.8	24.0	23.8	26.7	30.8
NO	59.8 (10.0)	54.1	25.2	52.5	48.3	51.4	33.4	45.6	49.7	49.8	47.1
CO	55.0 (12.5)	65.1	64.7	64.2	60.5	61.5	56.7	60.7	60.7	61.5	63.2
C_2H_4		79.4	79.3	86.2	83.5	86.8	78.7	78.3	79.0	81.3	83.3
H_2O	133.1 (13.5)	130.5	130.1	138.0	133.2	135.3	129.9	131.9	132.5	132.5	137.0
CH_3OH	155.0 (8.5)	147.0	146.6	154.2	147.4	148.8	143.9	147.9	147.6	147.8	152.8
C_6H_6	161.1 (13.5), *149.1 (10.3)*	143.4	145.0	153.2	151.2	157.4	150.3	155.8	146.7	151.1	154.6
CH_3OCH_3	165.0 (10.6)	152.2	151.6	158.7	151.1	153.4	148.6	153.1	152.0	152.8	157.9
NH_3	*159.1 (10.3)*	150.8	150.4	157.6	154.0	156.4	154.1	151.8	152.1	151.6	156.3
C_2H_5OH	163.5 (6.5)	158.0	157.4	166.9	160.6	162.1	154.9	159.3	159.2	170.1	165.1
CH_3NH_2	*165.5 (10.6)*	160.4	159.7	166.8	162.3	164.2	159.7	160.9	160.5	161.0	165.6
CH_3CHO	*166.3 (10.6)*	159.2	159.0	175.3	168.9	171.0	159.8	165.0	164.3	163.7	168.2
$C_2H_5CO_2H$	165.0 (6.0)	163.8	164.3	181.6	175.9	178.1	166.2	170.0	170.6	170.1	176.1
1-C_3H_7OH	170.3 (8.6)	163.4	164.6	175.3	166.6	169.5	159.9	164.8	166.0	168.4	174.8
2-C_3H_7OH	172.8 (7.5)	165.3	164.7	175.6	169.2	171.6	161.9	167.6	166.4	166.8	172.3
Pyrrole	177.4 (16.6)	158.1	158.2	166.3	163.6	169.0	158.7	161.9	158.9	160.1	167.6
C_6H_5OH	178.5 (16.1), *159.8 (10.7)*[c]	145.3	146.7	156.1	154.9	161.0	152.0	156.4	148.7	153.2	157.1
Pyridine	181.0 (14.5)	179.1	178.8	189.5	183.6	185.7	178.4	178.6	179.5	179.8	184.9
CH_3COCH_3	*182.6 (10.5)*	176.7	176.4	194.6	187.7	190.2	178.1	181.9	181.8	181.2	186.4
$CH_3COC_2H_5$	190.1 (7.0)	178.8	178.5	198.9	192.2	193.2	184.0	184.6	184.0	187.6	189.0
1-$C_3H_7NH_2$	197.8 (6.0)	180.8	180.0	188.7	183.9	185.4	179.7	181.2	180.8	181.9	188.5
Imidazole	210.8 (9.5), *195.1 (10.4)*	202.7	202.3	211.9	206.5	208.7	203.1	204.6	204.0	203.9	209.5
Uracil	211.5 (6.1)	194.9	194.7	212.4	204.9	209.7	196.3	200.6	199.5	198.8	204.7
Glycine	220.0 (8.0)	232.7	229.8	245.9	239.5	242.7	229.6	237.4	234.2	236.3	244.1
Adenine	226.1 (6.1)	199.8	200.4	204.9	196.7	200.3	202.4	208.6	201.1	201.6	208.0
$(CH_3)_2NCHO$	*208.5 (10.6)*	216.5	216.2	229.4	221.2	222.9	216.4	220.3	220.6	219.9	225.7
2-NH_2pyridine	237.8 (21.1)	214.9	214.7	220.0	212.4	216.1	218.0	212.2	214.6	214.0	220.8
$(CH_3OCH_2)_2$	241.2 (18.3), *229.0 (10.6)*	245.8	244.9	254.3	244.6	245.8	240.6	246.1	245.0	246.8	255.4
Proline	278.8 (9.7)	251.6	252.2	266.4	258.3	261.0	248.7	266.5	253.4	255.0	260.6
$HOC_2H_4NH_2$	289.5 (9.0)	255.8	254.5	264.4	257.8	259.6	253.0	254.3	257.2	253.4	261.8
12-crown-4	371.5 (51)	345.7	359.2	371.5	347.3	352.1	344.1	353.1	344.9		366.1
MAD vs. CBS[d]	30 values	7.1 (2.5)	8.3 (4.6)	3.1 (3.2)	4.4 (2.3)	3.7 (2.4)	8.2 (4.6)	8.3 (15.1)	5.6 (2.1)	4.8 (2.7)	2.2 (1.7)
MAD vs. exp[e]	25 values	11.8 (8.5)	13.0 (9.6)	9.9 (7.4)	10.7 (8.6)	9.5 (8.3)	12.6 (9.3)	10.3 (8.2)	10.7 (8.6)	10.5 (9.0)	8.6 (7.8)

[a] Experimental values including uncertainties in parentheses are taken from Table 1. ICR values are in italics.
[b] Geometry optimizations and frequency calculations use the 6-31G(d) basis set followed by single point calculations using 6–311 + G(2d, 2p) basis set. All values include zero point energy (with vibrational frequencies scaled by 0.9646) and counterpoise corrections for basis set superposition errors.
[c] Estimated from the methylated analogue.
[d] Mean absolute deviation from the complete basis set limit, HF/corr(DTQ), given in Table 8 (all values except 12-crown-4). Uncertainties in parentheses.
[e] Mean absolute deviation from the experimental data set (all values except 12-crown-4 and those having two entries). Uncertainties in parentheses.

Table 3
Counterpoise corrections for BSSE (kJ mol^{-1}) as a function of basis set size (no core correlation)[a]

	cc-pVDZ//cc-pVDZ	aug-cc-pVDZ//aug-cc-pVDZ	aug-cc-pVTZ//aug-cc-pVDZ	aug-cc-pVQZ//aug-cc-pVDZ
CO	10.3	8.5	8.7	8.4
C_2H_4	8.9	5.8	7.6	9.9
H_2O	22.9	12.6	8.6	9.5
CH_3OH	21.8	17.6	10.3	12.0
C_6H_6	17.9	19.3	18.4	19.3
NH_3	16.9	8.5	8.2	10.7
CH_3NH_2	18.1	16.2	10.7	12.7
CH_3CHO	18.9	21.7	11.1	13.5
$HOC_2H_4NH_2$	32.0	27.6	15.8	18.7
$(CH_2OCH_3)_2$	34.2	31.8	19.0	21.0
Average[b]	20.2 (8.1)	17.0 (8.5)	11.9 (4.3)	13.6 (4.5)

[a] MP2(full) calculations throughout using the basis sets indicated for single point energies//geometry optimizations.
[b] Uncertainties (one standard deviation) in parentheses.

smaller size of the lithium cation leads to M^+–L bond distances that are shorter, with greater electronic distortion of the ligand upon complexation. If the effect is primarily one of accurately describing the ligand in both the complex and its free state, then increasing the size of the basis set should enable a better description of the bond energies. Such an approach does not lead to appreciably better results, as illustrated in Table 3 for a representative set of the complexes of interest including both mono- and bidentate ligands. This table shows theoretical BSSE values for several ligands bound to Li^+ calculated using the correlation consistent polarized valence basis sets of Dunning [37] (cc-pVnZ where n = D, T, and Q) and where aug indicates that diffuse functions have been added to all atoms. Geometry optimizations are performed at either the MP2(full)/cc-pVDZ or MP2(full)/aug-cc-pVDZ levels, where the latter are used for single point energy calculations using the aug-cc-pVTZ and aug-cc-pVQZ basis sets. It can be seen that the magnitude of the BSSE values do not systematically decrease with increasing basis set size, as would be expected. Instead, VQZ values are generally larger than VTZ values and in two cases are greater than VDZ values. Clearly, even the large aug-cc-pVQZ basis sets are unable to properly describe the interactions of Li^+ with these ligands.

In considering the effects that a short Li^+–L bond distance might have on the complex, the lithium cation must also be considered. Note that the calculations of Table 3 are performed at the MP2(full) level, such that the 1s electrons are explicitly included in the calculation (as opposed to the default MP2(FC) frozen core level of theory). However, at sufficiently short metal cation–ligand bond distances, the closed-shell core electrons on the metal cation can interact repulsively with the closed-shell ligand. Such interactions can be relieved if the core electrons are permitted to polarize away from the ligand and to correlate with the ligand electrons. Standard basis functions do not include correlation functions on the core electrons, however, such basis sets have been developed as an enhancement of the correlation consistent basis sets of Dunning [56]. These correlation consistent polarized core/valence basis sets (cc-pCVnZ where n = D, T, and Q) extend the ideas of the original cc-pVnZ sets by including extra functions designed for core-core and core-valence correlation. In the following, the use of the cc-pCVnZ basis set on Li combined with cc-pVnZ or aug-cc-pVnZ basis sets on all other atoms will be designated by cc-pVnZ(Li-C) and aug-cc-pVnZ(Li-C). (Note that the cc-pCVnZ basis sets do not have diffuse functions available.)

Table 4
Counterpoise corrections for BSSE as a function of basis set size and geometry optimization for Li^+ (H_2O) without and with (Li-C) Li core correlation functions

Level of theory	cc-pVnZ			cc-pVnZ(Li-C)		
	cp[a]	D_0	cp-D_0[b]	cp[a]	D_0	cp-D_0[b]
MP2/cc-pVDZ (and vibs)	22.90	168.3	145.4	24.06	169.4	145.4
MP2/aug-cc-pVDZ//MP2/cc-pVDZ	11.10	139.8	128.7	3.05	132.2	129.2
MP2/aug-cc-pVTZ//MP2/cc-pVDZ	7.98	140.6	132.6	1.57	135.1	133.6
MP2/aug-cc-pVQZ//MP2/cc-pVDZ	8.94	144.1	135.2	0.77	136.8	136.0
CBS extrap, HF/corr(DTQ)		146.9			137.9	
MP2/aug-cc-pVDZ (and vibs)	12.58	139.5	127.0	3.03	131.8	128.8
MP2/aug-cc-pVTZ//MP2/aug-cc-pVDZ	8.64	140.2	131.6	1.56	134.8	133.3
MP2/aug-cc-pVQZ//MP2/aug-cc-pVDZ	9.54	144.0	134.4	0.77	136.4	135.7
CBS extrap, HF/corr(DTQ)		146.9			137.5	
MP2/aug-cc-pVTZ//MP2/aug-cc-pVTZ	8.57	140.9	132.3	1.59	135.0	133.4
MP2/aug-cc-pVQZ//MP2/aug-cc-pVTZ	9.50	144.6	135.2	0.79	136.7	135.9

[a] Counterpoise correction for BSSE effects on the bond dissociation energy.
[b] Counterpoise corrected bond dissociation energy.

The effect of adding core correlation functions to Li can be seen for the example of the $Li^+(H_2O)$ complex in Table 4. In contrast to the nonsystematic progression of counterpoise corrections for BSSE with increasing basis set size observed without core correlation functions on Li, the counterpoise corrections for calculations that include such polarization are much smaller and decrease nicely as the basis set size increases. Similar results (both with and without core correlation on Li) are obtained whether the geometry optimizations are performed at the MP2(full)/cc-pVDZ, MP2(full)/aug-cc-pVDZ, or MP2(full)/aug-cc-pVTZ levels. Likewise, similar results were obtained for the other complexes considered in Table 3. Significantly, it should be noticed that the D_0 values at the aug-cc-pVnZ, n = D, T, and Q, levels both with and without core correlation functions are *lower* than the LCA obtained for a CBS extrapolation (described in detail below), such that including counterpoise corrections for the BSSE increases the discrepancy with the CBS value. This is unusual because BSSE is generally a stabilizing contribution to the energy of the complex. This effect is also found for the many of the other Li^+ complexes, suggesting that the extensive electron correlation intrinsic in such tightly bound systems apparently results in the opposite behavior. In a few cases, such as the $Li^+(C_6H_6)$ complex, the uncorrected values either equal or are slightly larger than the CBS value, but counterpoise corrections increase the discrepancy with the CBS value, a result previously noted by Feller et al. for the $Li^+(C_6H_6)$ complex [43].

Clearly, the addition of core correlation functions to the Li center provides an improved description of the binding in the lithium cation complexes. To further explore how much core correlation should be included, several calculations were performed for the set of molecules in Table 3. These include both MP2(FC) and MP2(full) calculations using either no core correlation functions, core correlation functions on Li only, and core correlation functions on all heavy atoms (non-hydrogen). In all cases, the values were calculated using geometries and vibrational frequencies optimized using the aug-cc-pVDZ basis set followed by single point calculations using aug-cc-pVTZ and aug-cc-pVQZ basis sets. The values were then extrapolated to the CBS limit (using the HF/corr(DTQ) protocol described below) to eliminate basis set effects. The results are shown in Table 5. Not surprisingly, the MP2(FC) calculations are insensitive to the presence of core correlation functions. Mean absolute deviations (MADs) from the MP2(full)/cc-pCVnZ CBS results (where all heavy atoms have core correlation functions) are about 5 ± 2 kJ mol^{-1}. When no core correlation is used at the MP2(full) level, the MADs are much higher, about 24 ± 22 kJ mol^{-1}. The large changes associated with no core correlation can be traced to the difficulties presented in Table 3, namely, the CBS extrapolation is not behaving reasonably such that the LCAs obtained differ dramatically from the other approaches. In contrast, the difference between the values obtained with core correlation on only Li versus on all heavy atoms is only 0.3 ± 0.4 kJ mol^{-1}. Thus, addition of core correlation functions to all atoms does not improve the description of the bonding. This is understandable as it is the valence electrons on the ligands that are engaged in the bonding in the lithium cation complexes, and the core electrons on these atoms are consequently low in energy. In contrast, for Li^+, the 2s valence orbital is empty such that the only electrons present are the 1s core electrons. Correlation of the occupied 1s orbital allows these electrons to properly respond to the close approach of the closed shell ligand.

4.3. Effect of basis set size on geometry optimizations

In order to assess the size of the basis set needed to accurately describe lithium cation complexes, results were examined for geometry optimization at three levels: MP2(full)/cc-pVDZ(Li-C), MP2(full)/aug-cc-pVDZ(Li-C), and MP2(full)/aug-cc-pVTZ(Li-C) where core correlation on Li is used in all cases. Comparisons in Table 6 are made using single point calculations at the MP2(full)/aug-cc-pVQZ(Li-C) with counterpoise corrections for BSSE (nearly identical results are obtained without such corrections). Clearly the LCAs are not sensitive to the different basis sets used for the geometry optimization. MADs between experiment and the triple-ζ and two double-ζ levels of theory are essentially indistinguishable and differ by less than 0.5 kJ mol^{-1}. This is confirmed by a direct comparison among the three levels of theory, which

Table 5
Effect of including core correlation functions on calculated lithium cation affinities at 0 K in kJ mol^{-1}

Ligand	HF/corr(DTQ) extrapolation of MP2/aug-cc-pVnZ//MP2/aug-cc-pVDZ					
	FC/no core	FC/core(Li)	FC/core(all)	Full/no core	Full/core(Li)	Full/core(all)
CO	64.6	64.7	64.8	74.3	68.0	67.2
C_2H_4	81.0	81.1	81.3	96.4	84.2	84.2
H_2O	133.6	133.6	133.6	146.9	137.5	137.6
CH_3OH	149.0	148.9	148.9	165.4	153.2	153.2
C_6H_6	144.8	145.0	145.1	178.5	150.5	151.8
NH_3	152.8	152.9	152.9	170.0	157.3	156.9
CH_3NH_2	161.6	161.8	159.5	179.4	165.8	165.4
CH_3CHO	162.8	163.1	162.8	182.0	167.4	167.3
$(CH_2OCH_3)_2$	246.8	246.8	246.7	319.8	254.2	254.2
$HOC_2H_4NH_2$	255.1	255.2	255.1	326.6	262.4	262.4
MAD[a]	−4.8 (1.8)	−4.7 (1.8)	−5.0 (1.8)	23.9 (22.2)	0.3 (0.4)	

[a] Mean absolute deviation from full/core(all) values. Uncertainties (one standard deviation) in parentheses.

Table 6
Experimental and calculated lithium cation affinities at 0 K in kJ mol^{-1}[a]

Ligand	Experiment[b]	cc-pVDZ(Li-C)	aug-cc-pVDZ(Li-C)	aug-cc-pVTZ(Li-C)
Ar	32.8 (13.5)	25.4	25.9	26.4
CO	55.0 (12.5)	66.7	68.2	67.4
C_2H_4		83.6	83.4	84.1
H_2O	133.1 (13.5)	136.0	135.7	135.9
CH_3OH	155.0 (8.5)	151.9	151.5	151.6
C_6H_6	161.1 (13.5), *149.4 (10.3)*	150.7	150.6	150.5
CH_3OCH_3	165.0 (10.6)	156.2	156.6	156.5
NH_3	*159.1 (10.3)*	156.7	155.5	156.2
C_2H_5OH	163.5 (6.5)	163.5	163.1	163.3
CH_3NH_2	*165.5 (10.4)*	165.6	164.5	165.1
CH_3CHO	*166.3 (10.6)*	165.6	165.6	165.8
CH_3COCH_3	*182.6 (10.5)*	183.2	183.2	183.9
Imidazole	210.8 (9.5), *195.1 (10.4)*	207.6	207.7	208.1
Glycine	220.0 (8.0)	239.6	238.7	239.4
$(CH_3OCH_2)_2$	241.2 (18.3), *229.0 (10.6)*	251.4	251.4	252.7
Proline	278.8 (9.7)	261.3	260.4	262.1
$HOC_2H_4NH_2$	289.5 (9.0)	263.3	259.8	262.7
MAD vs. exp[c]		7.8 (8.6)	8.3 (9.2)	7.8 (8.6)
MAD vs. TZ[d]		0.5 (0.3)	0.7 (0.7)	

[a] Single point energies calculated at the MP2(full)/aug-cc-pVQZ(Li-C) level with geometries and ZPE corrections calculated at the MP2(full) level with the basis set shown (except that ZPE corrections for the aug-cc-pVTZ(Li-C) level are taken from cc-pVDZ(Li-C) values). BSSE corrections are also included.
[b] Experimental values including uncertainties in parentheses are taken from Table 1. ICR values are in italics.
[c] Mean absolute deviation from experiment excluding those having two values. Uncertainties in parentheses.
[d] Mean absolute deviation from aug-cc-pVTZ(Li-C) results. Uncertainties in parentheses.

exhibit MADs less than 1 kJ mol^{-1}, indicating that the shifts are not systematic and that the results at all three levels of theory are very similar. On the basis of this comparison, it is clear that geometry optimizations for lithium cation complexes can be accurately performed at the MP2(full)/cc-pVDZ(Li-C) level.

The trends observed in Table 5 are intriguing in that the MP2(FC) results are systematically low, whereas MP2(full)/(no core) values are systematically high. Table 7 compares the lithium cation–ligand bond lengths in these complexes calculated at these same levels of theory as well as MP2(full)/cc-pVDZ(Li-C) and MP2(full)/aug-cc-pVTZ(Li-C). The bond lengths at the MP2(full)/cc-pCVDZ (i.e., core correlation on all heavy atoms) and MP2(full)/aug-cc-pVDZ(Li-C) levels lead to nearly identical bond lengths, consistent with the very similar bond energies obtained. Likewise, MP2(full)/cc-pVDZ(Li-C) calculations give similar bond lengths, which differ by between −0.006 and 0.012 Å (except for CO where the difference is 0.029 Å). In contrast, the MP2(FC) calculations lead to bond lengths that are systematically larger by 0.010–0.015 Å. Hence, the weaker binding in the MP2(FC) calculations, Table 5, is a direct result of the lithium ion being too far away from the ligand, such that the electrostatic interaction is reduced. These results confirm that core correlation allows the 1s electrons on lithium to move away from the ligand, resulting in reduced Pauli repul-

Table 7
Calculated Li^+–L bond lengths (Å)[a]

Ligand	Li-X[b]	cc-pVDZ	aug-cc-pVDZ						aug-cc-pVTZ
		Full/core(Li)	FC/no core	FC/core(Li)	FC/core(all)	Full/no core	Full/core(Li)	Full/core(all)	Full/core(Li)
CO	C	2.249	2.231	2.229	2.229	2.152	2.220	2.220	2.174
C_2H_4	C(2)	2.419	2.437	2.430	2.428	2.391	2.416	2.415	2.368
H_2O	O	1.858	1.878	1.874	1.873	1.820	1.865	1.864	1.842
CH_3OH	O	1.839	1.854	1.853	1.852	1.805	1.843	1.843	1.820
C_6H_6	C(6)	2.382	2.394	2.394	2.392	2.324	2.3706	2.3705	2.311
NH_3	N	2.008	2.020	2.012	2.012	1.964	2.006	2.006	1.974
CH_3NH_2	N	2.004	2.008	2.005	2.004	1.951	1.996	1.995	1.968
CH_3CHO	O	1.804	1.812	1.814	1.811	1.767	1.801	1.800	1.776
$(CH_2OCH_3)_2$	O(2)	1.885	1.898	1.898	1.897	1.865	1.886	1.886	1.865
$HOC_2H_4NH_2$	O	1.883	1.898	1.897	1.896	1.862	1.886	1.885	1.863
	N	2.037	2.040	2.039	2.038	2.006	2.028	2.027	2.007
Avg dev[c]		+0.005 (0.010)	+0.014 (0.004)	+0.012 (0.004)	+0.011 (0.004)	−0.037 (0.014)	+0.0005 (0.0005)		−0.031 (0.013)

[a] All calculations use MP2(FC or full) and the indicated basis set with variations in whether core correlation is included on no atoms, only Li, or all heavy atoms. Diffuse functions (indicated by aug) are not present for atoms with core correlation.
[b] Indicates the atom to which the lithium cation is bound. Hapticity in parentheses.
[c] Average deviation from the MP2(full)/aug-cc-pCVDZ results (full/core(all)). Uncertainties (one standard deviation) in parentheses.

sion, shorter bond lengths, and a stronger interaction. Oddly, calculations at the MP2(full)/aug-cc-pVDZ level (no core correlation) give bond lengths that are considerably shorter than the MP2(full)/cc-pCVDZ results. These shorter bonds appear to be the result of the other basis functions being used to approximate core correlation, an effect that also leads to the large basis set superposition errors found in Table 3. These short bond lengths can explain why the bond energies are so much larger, but only if the Pauli repulsion between the 1s(Li) electrons and the ligand is underestimated compared to the other levels of theory. Finally, the bond lengths calculated at the MP2(full)/aug-cc-pVTZ(Li-C) level are also systematically smaller than the MP2(full)/aug-cc-pVDZ(Li-C) results. However, this does not lead to an appreciable change in the LCAs, as shown in Table 6. Apparently, there is a fine balance between the attractive ion-ligand electrostatic and the repulsive 1s(Li) core electron-ligand interactions that are handled differently at the double-ζ and triple-ζ levels.

4.4. Effect of the basis set size on energetics

The evolution of the 0 K LCAs with the size of the basis set was also examined. Results shown in Table 8 are for geometry optimizations and frequency analyses performed at the MP2(full)/cc-pVDZ(Li-C) level in most cases. Single point energy calculations at the MP2(full)/aug-cc-pVnZ(Li-C), n = D, T, and Q, levels were performed including BSSE corrections at the full counterpoise (cp) limit. The resulting values are then extrapolated to the CBS limit using the HF/corr(DTQ) protocol, described in detail in the next section. Parallel results were also obtained for geometry optimizations and frequency analyses performed at the MP2(full)/aug-cc-pVDZ(Li-C) level. Only the CBS extrapolated values are given in Table 8 for this level of theory because the results vary little as described below. Using the CBS extrapolated results for comparison, it can be seen that the MADs for values calculated without cp corrections are smaller than those that include cp corrections, except when the single point energy calculations do not include diffuse functions, cc-pVDZ(Li-C) results. In other words, the cp corrections fail to improve agreement with the CBS limit except when the basis set size is clearly too small. MADs for values without cp corrections decrease systematically with increasing basis set size: ∼4 kJ mol^{-1} for aug-cc-pVDZ(Li-C), ∼2 kJ mol^{-1} for aug-cc-pVTZ(Li-C), and ∼1 kJ mol^{-1} for aug-cc-pVQZ(Li-C). Values with cp corrections exhibit the same trend but are approximately twice as large. Comparison between the CBS extrapolated values for the cc-pVDZ(Li-C) and aug-cc-pVDZ(Li-C) geometry optimizations yield a MAD of only 0.8 kJ mol^{-1}, confirming the results found in the previous section that the cc-pVDZ(Li-C) basis is sufficient for geometry optimizations.

When these calculated values are compared to experiment, the resultant MADs exhibit the same general trends although now the best values are about 8 kJ mol^{-1}, with standard deviations of about 7 kJ mol^{-1}. The comparison between the CBS extrapolated values (cc-pVDZ(Li-C) geometry optimizations) and experiment is illustrated in Fig. 3. The general agreement is excellent, with the largest deviations occurring for the most strongly bound complexes, although large deviations that are both negative (glycine and $(CH_3OCH_2)_2$) and positive (adenine, 2-aminopyridine, proline, and $HOC_2H_4NH_2$) are observed. For more weakly bound species, the most notable outlier is phenol (positive deviation of 26 kJ mol^{-1}) although benzene also exhibits a larger than usual deviation of 10 kJ mol^{-1}. These observations may indicate that bidentate ligands and π-complexes in general are still not handled adequately at this level of theory, although the more strongly bound ligands may also be subject to more extensive experimental difficulties, as discussed above.

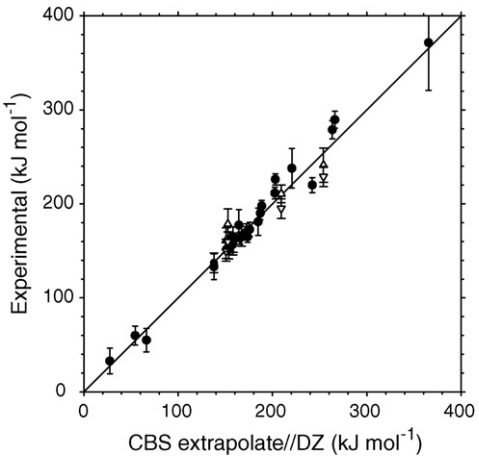

Fig. 3. Comparison of experimental LCAs and those calculated at the HF/corr(DTQ) CBS level. All values are 0 K enthalpies from Table 8, except for the theoretical value for 12-crown-4 which is a Schwartz4(DT) value from Table 9. Closed circles indicate the experimental data set of 26 values used for evaluation purposes. Open triangles indicate the four values for which GIBMS (up triangles) and ICR (down triangles) do not agree well.

4.5. Complete basis set extrapolations

The CBS extrapolation procedure used above is taken from a recipe outlined by Gdanitz et al. [57]. For the extrapolation at the Hartree–Fock (HF) level of theory, a three-point formula is used and employs energies calculated using aug-cc-pVnZ(Li-C), n = D, T, and Q. The HF limit energies were estimated using the empirical formula (2).

$$E_{HF}[\infty] = E_{HF}[x] - B\exp(-\alpha x) \quad (2)$$

In this extrapolation formula and those shown below, x is 2, 3, and 4, for the DZ, TZ, and QZ basis sets, respectively. When the three equations are combined to eliminate the parameters B and α, one obtains expression (3).

$$E_{HF}[\infty] = E_{HF}[4] + \frac{(E_{HF}[4] - E_{HF}[3])^2}{2E_{HF}[3] - E_{HF}[4] - E_{HF}[2]} \quad (3)$$

A recent study of Halkier et al. [58] shows that this formula reduces the maximum absolute error of the energies of eight first-row diatomics by a factor of three. For the correlation contribution, ΔE_{MP2} (=$E_{MP2} - E_{HF}$) is the correlation energy computed at the MP2(full) level of theory. The ΔE_{MP2} CBS limit is estimated using the extrapolation formulas proposed by

Table 8
Experimental and calculated lithium cation affinities at 0 K in kJ mol^{-1}[a]

Ligand	Experiment[b]	cp-DZ	DZ	cp-aug-DZ	aug-DZ	cp-aug-TZ	aug-TZ	cp-aug-QZ	aug-QZ	CBS[c]//DZ	CBS[c,d] //aug-DZ
Ar	32.8 (13.5)	17.7	25.0	20.3	23.0	24.4	26.8	25.4	27.4	27.5	28.2
NO	59.8 (10.0)	49.4	63.6	48.4	51.0	52.9	55.5	53.9	55.2	54.4	54.3
CO	55.0 (12.5)	62.5	72.7	62.0	65.1	66.2	69.7	66.7	68.2	66.4	68.0
C_2H_4		78.3	87.3	79.7	83.5	82.7	84.9	83.6	84.7	84.4	84.2
H_2O	133.1 (13.5)	145.4	169.4	129.2	132.2	133.6	135.1	136.0	136.8	137.9	137.5
CH_3OH	155.0 (8.5)	152.8	175.8	145.4	148.3	149.5	151.5	151.9	152.8	153.7	153.2
C_6H_6	161.1 (13.5), *149.1 (10.3)*	141.0	159.5	142.9	152.5	149.7	156.7	150.7	153.0	150.8	150.5
CH_3OCH_3	165.0 (10.6)	153.1	175.0	150.5	153.8	153.8	156.6	156.2	157.6	158.2	158.6
NH_3	*159.1 (10.3)*	164.2	182.0	150.7	154.3	154.9	156.2	156.7	157.5	158.5	157.3
C_2H_5OH	163.5 (6.5)	162.3	186.1	156.7	160.3	161.0	163.5	163.5	164.8	165.5	165.2
CH_3NH_2	*165.5 (10.6)*	166.6	185.9	160.4	163.9	163.9	165.9	165.6	166.5	167.0	165.8
CH_3CHO	*166.3 (10.6)*	158.0	177.7	158.3	161.7	163.2	166.0	165.6	167.0	167.4	167.4
$C_2H_5CO_2H$	165.0 (6.0)	167.5	187.3	164.3	168.6	168.7	172.1	171.5	173.1	173.6	173.2
1-C_3H_7OH	170.3 (8.6)	168.4	192.9	163.9	168.1	169.0	171.9	170.9	172.4	172.5	171.9
2-C_3H_7OH	172.8 (7.5)	168.1	191.9	164.1	167.9	168.3	171.0	172.8	173.7	175.7	173.6
Pyrrole	177.4 (16.6)	159.2	176.8	156.1	163.4	161.2	166.1	163.2	165.3	164.4	164.8
C_6H_5OH	178.5 (16.1), *159.8 (10.7)*[e]	145.4	165.0	144.9	154.5	150.8	157.8	152.6	155.2	152.6	154.5
Pyridine	181.0 (14.5)	179.2	196.1	178.3	182.2	182.1	185.2	183.8	185.2	184.8	184.9
CH_3COCH_3	*182.6 (10.5)*	194.4	174.9	175.7	179.4	180.8	184.3	183.2	185.0	185.1	184.7
$CH_3COC_2H_5$	190.1 (7.0)	176.0	194.5	178.1	181.8	183.6	187.1	185.8	187.3	187.1	187.4
1-$C_3H_7NH_2$	197.8 (6.0)	184.6	205.0	181.0	185.8	185.2	188.4	187.1	188.5	188.5	187.0
Imidazole	210.8 (9.5), *195.1 (10.4)*	206.0	224.2	201.5	205.1	205.9	208.4	207.6	209.1	209.2	209.3
Uracil	211.5 (6.1)	201.2	222.6	193.8	197.5	199.7	203.4	201.7	203.2	202.5	202.6
Glycine	220.0 (8.0)	244.7	276.1	231.9	237.8	236.5	240.6	239.6	241.5	242.2	241.2
Adenine	226.1 (6.1)	219.1	247.0	200.8	206.7	202.2	206.6	202.6	204.6	203.0	205.1
$(CH_3)_2NCHO$	*208.5 (10.6)*	215.3	238.4	214.9	218.5	220.0	223.0	222.4	223.9	224.2	224.4
$2NH_2$pyridine	237.8 (21.1)	224.3	250.4	216.2	221.5	218.7	222.8	219.8	221.6	220.5	219.7
$(CH_3OCH_2)_2$	241.2 (18.3), *229.0 (10.6)*	249.7	285.7	244.9	250.5	248.1	252.8	251.4	253.5	254.0	254.2
Proline	278.8 (9.7)	242.3	278.0	256.0	260.2	259.0	262.6	261.3	263.0	263.4	262.6
$HOC_2H_4NH_2$	289.5 (9.0)	271.9	305.3	256.2	261.7	259.8	263.4	263.3	264.9	266.1	262.4
12-crown-4	371.5 (51)	341.4	400.6	343.5	353.3	342.1	351.1				
MAD vs. CBS[f]	30 values	6.5 (4.4)	17.9 (10.4)	7.8 (2.0)	3.9 (1.7)	3.5 (1.7)	1.8 (1.5)	1.5 (0.8)	0.8 (0.7)		0.8 (0.8)
MAD vs. exp[g]	25 values	10.3 (8.3)	16.8 (12.1)	12.1 (7.9)	9.4 (6.9)	9.4 (7.9)	8.1 (7.3)	8.4 (7.8)	8.2 (7.3)	8.5 (7.3)	8.5 (7.7)

[a] All results, except as noted, refer to geometry optimizations at the MP2(full)/cc-pVDZ(Li-C) level followed by single point calculations at the MP2(full)/cc-pVnZ(Li-C), n = D, T, or Q, either with (aug) or without diffuse functions and with (cp) or without counterpoise corrections for BSSE. ZPE corrections were made using vibrational frequencies scaled by 0.9646 and calculated at the MP2(full)/cc-pVDZ(Li-C) level.

[b] Experimental values including uncertainties in parentheses taken from Table 1. ICR values in italics.

[c] Complete basis set (CBS) extrapolations performed using the HF/corr(DTQ) protocol described in the text.

[d] These CBS results utilize geometry optimizations at the MP2(full)/aug-cc-pVDZ(Li-C) level.

[e] Estimated from the methylated analogue.

[f] Mean absolute deviation from the complete basis set limit, CBS//DZ, HF/corr(DTQ) (all values except 12-crown-4). Uncertainties in parentheses.

[g] Mean absolute deviation from the experimental data set (all values except 12-crown-4 and those having two entries). Uncertainties in parentheses.

Schaefer and co-workers [59], namely Eq. (4).

$$\Delta E_{MP2}[\infty] = \Delta E_{MP2}[x] - a\left(x + \frac{1}{2}\right)^{-3} \quad (4)$$

In all cases, a two point extrapolation based on the aug-cc-pVTZ(Li-C) and aug-cc-pVQZ(Li-C) results is used, such that combining Eq. (4) with $x = 3$ and 4 and eliminating parameter a yields Eq. (5).

$$\Delta E_{MP2}[\infty] = \left(\frac{4.5^3 \Delta E_{MP2}[4] - 3.5^3 \Delta E_{MP2}[3]}{4.5^3 - 3.5^3}\right) = 1.8886\, \Delta E_{MP2}[4] - 0.8886\, \Delta E_{MP2}[3] \quad (5)$$

Schaefer and co-workers have demonstrated that this is the most accurate extrapolation method available for the correlation energy of general molecules [59]. Extrapolations for $\Delta E_{MP2}[\infty]$ using cc-pVDZ and cc-pVTZ results have generally been found to be unreliable [60]. The final CBS energy is then given by $E[\infty] = E_{HF}[\infty] + \Delta E_{MP2}[\infty]$ and is designated as HF/corr(DTQ) to emphasize that the HF and correlation energies are separately extrapolated.

An alternative extrapolation procedure used by Feller et al. [61] is based on a mixed exponential/Gaussian function of the form in Eq. (6).

$$E[n] = E[\infty] + B\, \exp[-(x-1)] + C\, \exp[-(x-1)^2] \quad (6)$$

When aug-cc-pVnZ, n = D, T, and Q, basis sets are used for an extrapolation ($x = 2$, 3, and 4), this equation reduces to Eq. (7).

$$E[\infty] = 1.676755E[4] - 0.711622E[3] + 0.034867E[2] \quad (7)$$

Note that here the energies used are the total energies.

On the basis of previous work by Schwartz [62], Martin has suggested both two (Schwartz4) and three (Schwartz6) point extrapolations of the total energy using Eqs. (8) and (9) [63].

$$E[\infty] = E[x] - a\left(x + \frac{1}{2}\right)^{-4} \quad (8)$$

$$E[\infty] = E[x] - a\left(x + \frac{1}{2}\right)^{-4} - b\left(x + \frac{1}{2}\right)^{-6} \quad (9)$$

Note that the form of these equations is similar to Eq. (4) but now the HF and correlation energies are not separately extrapolated. Eliminating the constants leads to the simplified results for Schwartz4(DT) of Eq. (10),

$$E[\infty] = 1.351914E[3] - 0.351914E[2] \quad (10)$$

Schwartz4(TQ) of Eq. (11),

$$E[\infty] = 1.577163E[4] - 0.577163E[3] \quad (11)$$

and for Schwartz6(DTQ) of Eq. (12).

$$E[\infty] = 1.913310E[4] - 0.988315E[3] + 0.075005E[2] \quad (12)$$

These various CBS extrapolation procedures are compared in Table 9. It can be seen that the three-point extrapolations agree with one another very well, with MADs of 0.1 and 0.2 kJ mol^{-1} for the Schwartz6(DTQ) and Feller(DTQ) procedures, respectively, compared to the somewhat more complicated HF/corr(DTQ). These differences are much smaller than those obtained by changing the level used for the geometry optimizations (MAD of 0.8 kJ mol^{-1}). In addition, the Schwartz4(TQ) two-point extrapolation also gives very good agreement (MAD of 0.3 kJ mol^{-1}) with HF/corr(DTQ), and the Schwartz4(DT) results deviate from the three-point extrapolations by only 2 kJ mol^{-1}. Interestingly, this latter approach gives the best comparison to experiment, although only marginally, in part because it provides somewhat higher values than the other extrapolation procedures. Overall, the agreement between any of these CBS results and experiment are essentially identical.

As noted above, Feller et al. [43] have previously used the Feller(DTQ) approach (including core correlation effects) in calculating the LCA of $Li^+(C_6H_6)$. The value they determined of 151.0 kJ mol^{-1} is the same as our Feller(DTQ) value of 151.2 kJ mol^{-1}, especially once it is realized that the literature value includes a −0.2 kJ mol^{-1} correction from higher order correlation effects estimated from CCSD(T) calculations. This comparison suggests that such higher order correlation effects are not needed to achieve the best computational results. To confirm this result for the other complexes considered here, CCSD(T, full)/aug-cc-pVDZ(Li-C)//MP2(full)/aug-cc-pVDZ(Li-C) calculations of the LCAs were performed for all complexes but 12-crown-4 and the correction from MP2 to CCSD(T) values extracted directly from these computed results. These results are detailed in Table 10. For the smallest complexes (Ar, CO, NO, H_2O, and NH_3), it was verified that use of a triple-ζ level, CCSD(T)/aug-cc-pVTZ(Li-C), instead of double-ζ basis set changed the corrections by less than one kJ mol^{-1} (the average difference was 0.5 ± 0.3 kJ mol^{-1}). These CCSD(T) calculations indicate that the corrections for higher order correlation lie between −1.2 and 2.7 kJ mol^{-1} (with an average of 0.6 ± 1.2 kJ mol^{-1}) for all but two complexes, Li^+(CO) and Li^+(NO). In these two cases, these higher order correlation corrections improve the agreement between experiment and theory for Li^+(CO), 55.0 ± 12.5 and 61.2 kJ mol^{-1}, respectively, for HF/corr(DTQ) with CCSD(T), but worsen the agreement for Li^+(NO), 59.8 ± 10.0 and 49.4 kJ mol^{-1}, respectively, for HF/corr(DTQ) with CCSD(T). If these higher order correlation effects are included in the HF/corr(DTQ) CBS bond energies, the comparison to the experimental data set (25 values) changes the MAD from 8.5 ± 7.3 kJ mol^{-1} to 8.6 ± 7.5 kJ mol^{-1}, clearly indicating that their influence is minor.

4.6. Accurate approaches

Complete basis set extrapolations utilizing two and three-point extrapolations from single point energies calculated at the MP2(full)/aug-cc-pVnZ(Li-C)//MP2(full)/cc-pVDZ(Li-C) levels where n = D, T, and Q appear to provide reasonable agreement between experiment and theory for most of the lithium cation complexes considered here. This approach is computationally intensive because of the use of the large aug-cc-pVQZ(Li-C) basis set and is very time consuming for

Table 9
Comparison of complete basis set extrapolation methods for lithium cation affinities at 0 K in kJ mol^{-1}[a]

Ligand	Experiment[b]	HF/corr (DTQ)	Feller (DTQ)	Schwartz4 (DT)	Schwartz4 (TQ)	Schwartz6 (DTQ)
Ar	32.8 (13.5)	27.5	27.7	28.2	27.8	27.7
NO	59.8 (10.0)	54.4	54.8	57.1	55.0	54.6
CO	55.0 (12.5)	66.4	67.0	71.3	67.3	66.4
C_2H_4		84.4	84.5	85.3	84.6	84.4
H_2O	133.1 (13.5)	137.9	137.8	136.2	137.7	138.0
CH_3OH	155.0 (8.5)	153.7	153.7	152.6	153.6	153.8
C_6H_6	161.1 (13.5), *149.1 (10.3)*	150.8	151.2, 151.0[c]	156.8	151.6	150.5
CH_3OCH_3	165.0 (10.6)	158.2	158.3	157.6	158.2	158.4
NH_3	*159.1 (10.3)*	158.5	158.3	156.9	158.3	158.6
C_2H_5OH	163.5 (6.5)	165.5	165.5	164.6	165.5	165.7
CH_3NH_2	*165.5 (10.6)*	167.0	166.9	166.6	166.9	167.0
CH_3CHO	*166.3 (10.6)*	167.4	167.4	167.6	167.5	167.5
$C_2H_5CO_2H$	165.0 (6.0)	173.6	173.6	173.4	173.6	173.7
1-C_3H_7OH	170.3 (8.6)	172.5	172.6	173.2	172.6	172.5
2-C_3H_7OH	172.8 (7.5)	175.7	175.4	172.2	175.2	175.9
Pyrrole	177.4 (16.6)	164.4	164.7	167.1	164.8	164.4
C_6H_5OH	178.5 (16.1) *159.8 (10.7)*[d]	152.6	153.3	158.9	153.6	152.5
Pyridine	181.0 (14.5)	184.8	185.1	186.3	185.2	184.9
CH_3COCH_3	*182.6 (10.5)*	185.1	185.2	186.1	185.4	185.2
$CH_3COC_2H_5$	190.1 (7.0)	187.1	187.2	188.9	187.4	187.1
1-$C_3H_7NH_2$	197.8 (6.0)	188.5	188.5	189.3	188.6	188.4
Imidazole	210.8 (9.5), *195.1 (10.4)*	209.2	209.4	209.6	209.4	209.4
Uracil	211.5 (6.1)	202.5	202.9	205.4	203.2	202.7
Glycine	220.0 (8.0)	242.2	242.0	241.5	242.0	242.2
Adenine	226.1 (6.1)	203.0	203.2	206.6	203.4	202.8
$(CH_3)_2NCHO$	*208.5 (10.6)*	224.2	224.4	224.6	224.4	224.4
$2NH_2$pyridine	237.8 (21.1)	220.5	220.8	223.3	220.9	220.4
$(CH_3OCH_2)_2$	241.2 (18.3), *229.0 (10.6)*	254.0	254.0	253.5	254.0	254.1
Proline	278.8 (9.7)	263.4	263.2	263.5	263.2	263.2
$HOC_2H_4NH_2$	289.5 (9.0)	266.1	265.8	264.0	265.7	266.1
12-crown-4	371.5 (51)			365.2		
MAD vs. HF/corr[e]			0.2 (0.2)	1.8 (1.7)	0.3 (0.3)	0.1 (0.1)
MAD vs. exp[f]		8.5 (7.3)	8.4 (7.3)	8.1 (7.3)	8.4 (7.3)	8.5 (7.4)

[a] All values use geometry optimizations and vibrational frequencies calculated at the MP2(full)/cc-pVDZ(Li-C) level. The values shown are extrapolated from the designated aug-cc-pVnZ(Li-C), n = D, T, Q, single point energies as described in the text.
[b] Experimental values including uncertainties in parentheses taken from Table 1. ICR values in italics.
[c] Value from Feller et al. [43] which includes −0.2 kJ mol^{-1} in higher order correlation effects estimated from CCSD(T) calculations.
[d] Estimated from the methylated analogue.
[e] Mean absolute deviation vs. HF/corr(DTQ) CBS extrapolated values. Uncertainties in parentheses.
[f] Mean absolute deviation vs. experimental values (except 12-crown-4 and those having two values). Uncertainties in parentheses.

the larger complexes considered here. Therefore, it would be desirable to determine a lower level of theory that provides reasonable predictions for the thermochemistry of lithium cation complexes while correctly including the core correlation effects on lithium noted above. Table 2 compares the conventional approaches with the HF/corr(DTQ) CBS results. The best and only results comparable to the CBS approach used here are those from G3 theory, which is also computationally intensive. Intriguingly MP2 results excluding counterpoise corrections for BSSE perform almost as well. However, this must be partially serendipitous because these results do not consider the core correlation effects that are clearly important in these systems. Nevertheless, this observation can be explored more thoroughly by examining Table 8, which shows that excluding cp corrections leads to better agreement with the CBS limit when an adequately large basis set is used. Note that the MP2(full)/aug-cc-pVTZ(Li-C)//MP2(full)/cc-pVDZ(Li-C) level of theory without cp corrections gives fairly good agreement with the CBS limit (MAD of 1.8 ± 1.5 kJ mol^{-1} and an average deviation of −0.2 ± 2.4 kJ mol^{-1}), and is a level of theory comparable to the MP2(full)/6-311 + G(2d,2p)//MP2(full)/6-31G(d) level previously proposed to examine sodium cation complexes [1,64]. These results are generally slightly lower than the CBS values (by an average of about 0.2%), but the largest deviations (5–6 kJ mol^{-1}) occur for the π-bound complexes of benzene, phenol, and pyrrole where the CBS values are lower. In these cases, the lower level of theory agrees with experiment better than the CBS limit. This is one reason that this level of theory provides nearly the best comparison with experiment among all of the levels examined in Table 8. We propose that this level of theory should provide an adequate description of most lithium cation complexes at a modest computational cost. An attractive alternative that involves little additional computational effort is to calculate MP2(full)/aug-

Table 10
Higher order correlation corrections for lithium cation affinities at 0 K in kJ mol^{-1} [a]

Ligand	MP2(full)/DZ[a]	CCSD(T, full)/DZ[b]	Δ[c]	MP2(full)/TZ[a]	CCSD(T, full)/TZ[b]	Δ[c]
Ar	24.54	24.98	0.40	28.73	29.01	0.28
NO	54.12	49.07	−5.05	58.24	53.72	−4.52
CO	70.08	64.85	−5.23	75.02	70.37	−4.65
C_2H_4	87.79	87.27	−0.52			
H_2O	139.52	139.50	−0.02	142.67	143.05	0.38
CH_3OH	154.02	153.66	−0.36			
C_6H_6	157.77	156.81	−0.96			
CH_3OCH_3	159.35	159.10	−0.26			
NH_3	163.07	162.42	−0.65	164.91	165.08	0.17
C_2H_5OH	165.19	164.99	−0.20			
CH_3NH_2	171.12	170.66	−0.46			
CH_3CHO	167.18	168.58	1.40			
$C_2H_5CO_2H$	173.67	175.93	2.27			
1-C_3H_7OH	174.40	174.54	0.14			
2-C_3H_7OH	172.22	172.01	−0.21			
Pyrrole	150.07	151.35	1.28			
C_6H_5OH	140.99	142.05	1.06			
Pyridine	169.51	171.29	1.78			
CH_3COCH_3	184.18	185.67	1.49			
$CH_3COC_2H_5$	166.71	169.41	2.70			
1-$C_3H_7NH_2$	173.42	173.87	0.45			
Imidazole	211.55	211.37	−0.18			
Uracil	182.92	185.34	2.42			
Glycine	226.73	229.09	2.37			
Adenine	215.59	217.51	1.93			
$(CH_3)_2NCHO$	225.67	227.86	2.19			
$2NH_2$pyridine	209.41	209.93	0.51			
$(CH_3OCH_2)_2$	239.21	239.67	0.46			
Proline	248.39	247.18	−1.21			
$HOC_2H_4NH_2$	274.05	273.36	−0.68			

[a] Bond energy calculated at the MP2(full)/aug-cc-pVnZ(Li-C) level.
[b] Bond energy calculated at the CCSD(T, full)/aug-cc-pVnZ(Li-C)//MP2(full)/aug-cc-pVDZ(Li-C) level. No zero point or counterpoise corrections.
[c] Difference between the CCSD(T) and MP2(full) bond energies.

cc-pVnZ(Li-C)//MP2(full)/cc-pVDZ(Li-C) values for both n = D and T and use the Schwartz4(DT) extrapolation to give a CBS value. Comparison with the HF/corr(DTQ) results in Table 9 shows that this method yields results that are slightly higher (by an average of about 0.4%), with the largest deviations (5–6 kJ mol^{-1}) again occurring for benzene and phenol. Overall, it is notable that the Schwartz4(DT) and MP2(full)/aug-cc-pVTZ(Li-C)//MP2(full)/cc-pVDZ(Li-C) values generally bracket the HF/corr(DTQ) results.

As a double check, the LCAs computed from B3LYP/aug-cc-pVTZ(Li-C)//B3LYP/cc-pVDZ(Li-C) calculations (including ZPE but not counterpoise corrections for BSSE) for all of these complexes are compared to experiment, which produces a MAD of 10.9 ± 7.5 kJ mol^{-1}. In addition, the B3LYP values are systematically higher than the HF/corr(DTQ) CBS limits, with a MAD of 5 ± 4 kJ mol^{-1}. Thus, the MP2(full) approach provides better agreement with experiment and the CBS limits than comparable B3LYP calculations.

4.7. Assessment of literature data

Having examined the various theoretical approaches, it is useful to now go back and reassess the literature values available. For the most part, advanced theory and experimental LCAs agree well. As noted above, four values from our experimental data set were excluded in our comparisons because of the discrepant GIBMS and ICR values. For two of these, imidazole and $(CH_3OCH_2)_2$, the GIBMS values agree better with theory, Table 8, with the ICR values being too low and outside experimental error. Indeed, the theory value for $(CH_3OCH_2)_2$ is higher than the GIBMS experimental value (but within experimental error), one of the few systems where this is the case. For the other two systems, benzene and phenol, the ICR values agree better with theory, with the GIBMS values being too high although within experimental error for benzene. It is interesting that the three π-complexes, benzene, pyrrole, and phenol, all exhibit this same trend, with GIBMS experiments being higher than theory by 10.3, 13.0, and 25.9 kJ mol^{-1}, respectively. In these systems, the lithium cation must interact with a diffuse π cloud, which may require that more diffuse basis functions are necessary to describe the cation-π interaction appropriately.

The other systems that have larger than usual discrepancies between theory and experiment include those that bind most tightly: glycine (GIBMS lower than theory by 22 kJ mol^{-1}), adenine (GIBMS higher than theory by 23 kJ mol^{-1}), 2-aminopyridine (GIBMS higher than theory by 17 kJ mol^{-1}, but within the experimental error of 21 kJ mol^{-1}), proline (GIBMS higher than theory by 15 kJ mol^{-1}), and $HOC_2H_4NH_2$ (GIBMS

higher than theory by 24 kJ mol^{-1}). Alternate values available in the literature from kinetic method measurements for glycine and proline, Table 1, are in worse agreement with theory. Those for uracil and adenine agree with the GIBMS values, although this is somewhat fortuitous as they are referenced to the LCA for glycine taken from kinetic method experiments. The two ICR values with large discrepancies compared to theory, $(CH_3)NCHO$ and $(CH_3OCH_2)_2$, are lower than the theoretical values by 16 and 25 kJ mol^{-1}, respectively. In all of these systems, the ligands are bidentate, which could mean that theory is having difficulty with the strong ligand distortions and more diffuse bonding involved in these complexes. These strong bonds also lead to large CID thresholds, which could lead to unexpected difficulties in the experimental analysis, as discussed above, although such difficulties are not encountered for comparable Cu^+–L complexes that have even stronger bonds.

5. Conclusions

An assessment of the discrepancy between experimental and theoretical LCAs over a large range shows that core correlation effects on the lithium cation are appreciable. Advanced computations that include such effects as well as CBS extrapolations provide larger LCAs than most other methods, although serendipitously, there are theoretical approaches that perform almost as well. Because the CBS approach requires use of the computationally intensive aug-cc-pVQZ(Li-C) basis set, we recommend that an adequate level of theory is provided by a MP2(full)/aug-cc-pVTZ(Li-C)//MP2(full)/cc-pVDZ(Li-C) approach perhaps augmented by the Schwartz4(DT) CBS extrapolation approach.

These theoretical approaches accurately describe the binding energies of most of the complexes examined here, i.e., 20 out of 29 systems are within experimental error and another 3 are just outside the experimental error limits. However, several molecules still exhibit discrepancies between theory and experiment. Not surprisingly, these are usually localized among the larger systems that often involve multidentate interactions with the lithium cation. Analysis of the experimental approach of threshold collision-induced dissociation provides no obvious reasons for such difficulties, although difficulties with collecting the light lithium ion may lead to CID cross-sections that are not accurately analyzed for their true thermodynamic threshold. These systems would be useful to examine using alternative experimental approaches (for example, by ligand exchange reactions) to clarify whether theory or experiment introduces the most error.

Acknowledgement

This work is supported by the National Science Foundation, Grants. CHE-0518262 (MTR) and CHE-0451477 (PBA). The authors thank Anita Orendt for her considerable help with running some of these calculations at the University of Utah Center for High Performance Computing (CHPC) and Nalaka S. Rannulu for his help running calculations on the GRID at Wayne State. Jack Simons is thanked for a number of illuminating conversations. A grant of computer time from the CHPC, partially supported by NIH-NCRR Grant #1S1ORR17214, is gratefully acknowledged. Some basis sets were obtained from the Extensible Computational Chemistry Environment Basis Set Database, Version 02/02/06, and the Basis Set Library as developed and distributed by the Molecular Science Computing Facility, Environmental and Molecular Sciences Laboratory which is part of the Pacific Northwest Laboratory, P.O. Box 999, Richland, Washington 99352, USA, and funded by the U.S. Department of Energy. The Pacific Northwest Laboratory is a multi-program laboratory operated by Battelle Memorial Institute for the U.S. Department of Energy under contract DE-AC06-76RLO 1830.

References

[1] P.B. Armentrout, M.T. Rodgers, J. Phys. Chem. A 104 (2000) 2238.
[2] M.B. More, E.D. Glendening, D. Ray, D. Feller, P.B. Armentrout, J. Phys. Chem. 100 (1996) 1605.
[3] D. Ray, D. Feller, M.B. More, E.D. Glendening, P.B. Armentrout, J. Phys. Chem. (1996) 16116.
[4] M.T. Rodgers, P.B. Armentrout, J. Phys. Chem. A 101 (1997) 1238.
[5] M.T. Rodgers, P.B. Armentrout, J. Phys. Chem. A 101 (1997) 2614.
[6] D. Walter, M.R. Sievers, P.B. Armentrout, Int. J. Mass Spectrom. 173 (1998) 93.
[7] M.T. Rodgers, P.B. Armentrout, Int. J. Mass Spectrom. 185–187 (1999) 359.
[8] M.T. Rodgers, P.B. Armentrout, J. Am. Chem. Soc. 122 (2000) 8548.
[9] J.C. Amicangelo, P.B. Armentrout, J. Phys. Chem. A 104 (2000) 11420.
[10] R. Amunugama, M.T. Rodgers, Int. J. Mass Spectrom. 195–196 (2000) 439.
[11] M.T. Rodgers, J.R. Stanley, R. Amunugama, J. Am. Chem. Soc. 122 (2000) 10969.
[12] M.T. Rodgers, J. Phys. Chem. A 105 (2001) 8145.
[13] H. Huang, M.T. Rodgers, J. Phys. Chem. A 106 (2002) 4277.
[14] R. Amunugama, M.T. Rodgers, J. Phys. Chem. A 106 (2002) 5529.
[15] R. Amunugama, M.T. Rodgers, J. Phys. Chem. A 106 (2002) 9092.
[16] R. Amunugama, M.T. Rodgers, J. Phys Chem. A 106 (2002) 9718.
[17] R. Amunugama, M.T. Rodgers, Int. J. Mass Spectrom. 222 (2003) 431.
[18] R. Amunugama, M.T. Rodgers, Int. J. Mass Spectrom. 227 (2003) 1.
[19] R. Amunugama, M.T. Rodgers, Int. J. Mass Spectrom. 227 (2003) 339.
[20] Z. Yang, M.T. Rodgers, J. Am. Chem. Soc. 126 (2004) 16217.
[21] C. Ruan, Z. Yang, N. Hallowita, M.T. Rodgers, J. Phys. Chem. A 109 (2005) 11539.
[22] Z. Yang, M.T. Rodgers, Int. J. Mass Spectrom. 241 (2005) 225.
[23] Z. Yang, M.T. Rodgers, J. Phys. Chem. A 1101 (2006) 1455.
[24] R.M. Moision, P.B. Armentrout, J. Phys. Chem. A 110 (2006) 3933.
[25] R.M. Moision, P.B. Armentrout, work in progress.
[26] B. Stzaray, C. Iceman, P.B. Armentrout, work in progress.
[27] R.L. Woodin, J.L. Beauchamp, J. Am. Chem. Soc. 100 (1978) 501.
[28] I. Džidić, P. Kebarle, J. Phys. Chem. 74 (1970) 1466.
[29] R.W. Taft, F. Anvia, J.-F. Gal, S. Walsh, M. Capon, M.C. Holmes, K. Hosn, G. Oloumi, R. Vasanwala, S. Yazdani, Pure Appl. Chem. 62 (1990) 17.
[30] P. Burk, I.A. Koppel, I. Koppel, R. Kurg, J.-F. Gal, P.-C. Maria, M. Herreros, R. Notario, J.-L.M. Abboud, F. Anvia, R.W. Taft, J. Phys. Chem. A 104 (2000) 2824.
[31] L.A. Curtiss, K. Raghavachari, G.W. Trucks, J.A. Pople, J. Chem. Phys. 94 (1991) 7221.
[32] G. Bojesen, T. Breindahl, U.N. Andersen, Org. Mass Spectrom. 28 (1993) 1448.
[33] B.A. Cerda, C. Wesdemiotis, J. Am. Chem. Soc. 118 (1996) 11884.
[34] W.Y. Feng, S. Gronert, C.B. Lebrilla, J. Phys. Chem. A 107 (2003) 405.
[35] J.E. del Bene, J. Phys. Chem. 88 (1984) 5927.
[36] J.E. del Bene, J. Phys. Chem. 100 (1996) 6284.

[37] T.H. Dunning Jr., J. Chem. Phys. 90 (1989) 1007;
R.A. Kendall, T.H. Dunning Jr., R.J. Harrison, J. Chem. Phys. 96 (1992) 6796.
[38] M. Remko, K.R. Liedl, B.M. Rode, J. Phys. Chem. A 102 (1998) 771.
[39] M.R. Nyden, G.A. Petersson, J. Chem. Phys. 75 (1981) 1843;
G.A. Petersson, M.A. Al-Laham, J. Chem. Phys. 94 (1991) 6081;
G.A. Petersson, T. Tensfeldt, J.A. Montgomery, J. Chem. Phys. 94 (1991) 6091;
J.A. Montgomery, J.W. Ochterski, G.A. Petersson, J. Chem. Phys. 101 (1994) 5900.
[40] F.M. Siu, M.L. Ma, C.W. Tsang, J. Chem. Phys. 114 (2001) 7045.
[41] L.A. Curtiss, K. Raghavachari, P.C. Redfern, V. Rassolov, J.A. Pople, J. Chem. Phys. 109 (1998) 7764.
[42] J.B. Nicholas, B.P. Hay, D.A. Dixon, J. Phys. Chem. A 103 (1999) 1394.
[43] D. Feller, D.A. Dixon, J.B. Nicholas, J. Phys. Chem. A (2000) 11414.
[44] J.M. Vollmer, A.K. Kandalam, L.A. Curtiss, J. Phys. Chem. A 106 (2002) 9533.
[45] L.A. Curtiss, P.C. Redfern, K. Raghavachari, V. Rassolov, J.A. Pople, J. Chem. Phys. 110 (1999) 4703.
[46] Gerlich, D., in: Ng, C.-Y., Baer, M. (Eds.). State-Selected and State-to-State Ion-Molecule Reaction Dynamics. Part I. Experiment, vol. 82. Adv. Chem. Phys (1992) 1.
[47] M.T. Rodgers, K.M. Ervin, P.B. Armentrout, J. Chem. Phys. 106 (1997) 4499.
[48] M.J. Frisch, G.W. Trucks, H.B. Schlegel, G.E. Scuseria, M.A. Robb, J.R. Cheeseman, J.A. Montgomery Jr., T. Vreven, K.N. Kudin, J.C. Burant, J.M. Millam, S.S. Iyengar, J. Tomasi, V. Barone, B. Mennucci, M. Cossi, G. Scalmani, N. Rega, G.A. Petersson, H. Nakatsuji, M. Hada, M. Ehara, K. Toyota, R. Fukuda, J. Hasegawa, M. Ishida, T. Nakajima, Y. Honda, O. Kitao, H. Nakai, M. Klene, X. Li, J.E. Knox, H.P. Hratchian, J.B. Cross, C. Adamo, J. Jaramillo, R. Gomperts, R.E. Stratmann, O. Yazyev, A.J. Austin, R. Cammi, C. Pomelli, J.W. Ochterski, P.Y. Ayala, K. Morokuma, G.A. Voth, P. Salvador, J.J. Dannenberg, V.G. Zakrzewski, S. Dapprich, A.D. Daniels, M.C. Strain, O. Farkas, D.K. Malick, A.D. Rabuck, K. Raghavachari, J.B. Foresman, J. Ortiz, Q. Cui, A.G. Baboul, S. Clifford, J. Cioslowski, B.B. Stefanov, G. Liu, A. Liashenko, P. Piskorz, I. Komaromi, R.L. Martin, D.J. Fox, T. Keith, M.A. Al-Laham, C.Y. Peng, A. Nanayakkara, M. Challacombe, P.M.W. Gill, B. Johnson, W. Chen, M.W. Wong, C. Gonzalez, J.A. Pople, Gaussian 03, Revision B.02, Gaussian, Inc., Pittsburgh, PA, 2003.
[49] A.D. Becke, J. Chem. Phys. 98 (1993) 5648.
[50] C. Lee, W. Yang, R.G. Parr, Phys. Rev. B 37 (1988) 785.
[51] J.P. Perdew, Phys. Rev. B 33 (1986) 8822.
[52] C. Adamo, V. Barone, J. Chem. Phys. 108 (1998) 664.
[53] Oddly, vibrational frequency analyses of NO using the MP2 approach with any basis set gave a frequency too high by about a factor of two compared with the experimental value, whereas other approaches performed as expected. This anomaly propagated to the Li^+(NO) complex such that ZPE corrections to the LCA of NO calculated using MP2 methods are incorrect (for unknown reasons). Hence, ZPE corrections for the Li^+(NO) complex use the vibrational frequencies calculated at the B3LYP/6-3 lG(d) level throughout the manuscript.
[54] S.F. Boys, R. Bernardi, Mol. Phys. 19 (1979) 553.
[55] F.B. Van Duijneveldt, J.G.C.M. van Duijneveldt-van de Rijdt, J.H. van Lenthe, Chem. Rev. 94 (1994) 1873.
[56] D.E. Woon, T.H. Dunning Jr., J. Chem. Phys. 103 (1995) 4572.
[57] R.J. Gdanitz, W. Cardoen, T.L. Windus, J. Simons, J. Phys. Chem. A 108 (2004) 515.
[58] A. Halkier, T. Helgaker, P. Jørgensen, W. Klopper, J. Olsen, Chem. Phys. Lett. 302 (1999) 437.
[59] E.F. Valeev, W.D. Allen, R. Hernandez, C.D. Sherrill, H.F. Schaefer, J. Chem. Phys. 118 (2003) 8594.
[60] A. Halkier, T. Helgaker, P. Jørgensen, W. Klopper, H. Koch, J. Olsen, A.K. Wilson, Chem. Phys. Lett. 286 (1998) 243.
[61] D. Feller, D.A. Dixon, J.B. Nicholas, J. Phys. Chem. A 104 (2000) 11414.
[62] C. Schwartz, in: B.J. Alder (Ed.), Methods in Computational Physics, vol. 2, Academic Press, New York, 1963.
[63] J.M.L. Martin, Chem. Phys. Lett. 259 (1996) 669.
[64] S. Hoyau, K. Norrman, T.B. McMahon, G. Ohanessian, J. Am. Chem. Soc. 121 (1999) 8864.